

Nestin-Linked Green Fluorescent Protein Transgenic Nude Mouse for Imaging Human Tumor Angiogenesis

Yasuyuki Amoh,^{1,2,3} Meng Yang,¹ Lingna Li,¹ Jose Reynoso,¹ Michael Bouvet,² Abdool R. Moossa,² Kensei Katsuoka,² and Robert M. Hoffman^{1,2}

¹AntiCancer, Inc.; ²Department of Surgery, University of California San Diego, San Diego, California; and ³Department of Dermatology, Kitasato University School of Medicine, Sagamihara, Japan

Abstract

We report here a novel transgenic nude mouse for the visualization of human tumor angiogenesis. We have recently shown that the neural stem cell marker nestin is expressed in hair follicle stem cells and blood vessel networks in the skin of C57/B6 transgenic mice with nestin regulatory element-driven green fluorescent protein (ND-GFP). Others have shown ND-GFP is expressed in the brain, pancreas, and testes in these mice. In the present study, the nestin ND-GFP gene was crossed into nude mice on the C57/B6 background to obtain ND-GFP nude mice. ND-GFP was expressed in the brain, spinal cord, pancreas, stomach, esophagus, heart, lung, blood vessels of glomeruli, blood vessels of skeletal muscle, testes, hair follicles, and blood vessel network in the skin of ND-GFP nude mice. Human lung cancer, pancreatic cancer, and colon cancer cell lines as well as a murine melanoma cell line and breast cancer tumor cell line expressing red fluorescent protein were implanted orthotopically, and a red fluorescent protein-expressing human fibrosarcoma was implanted s.c. in the ND-GFP nude mice. These tumors grew extensively in the ND-GFP mice. ND-GFP was highly expressed in proliferating endothelial cells and nascent blood vessels in the growing tumors, visualized by dual-color fluorescence imaging. Results of immunohistochemical staining showed that CD31 was expressed in the ND-GFP-expressing nascent blood vessels. The ND-GFP transgenic nude mouse model enables the visualization of nascent angiogenesis in human and mouse tumor progression. These results suggest that this model is useful for the imaging of the angiogenesis of human as well as rodent tumors and visualization of the efficacy of angiogenic inhibitors. (Cancer Res 2005; 65(12): 5352-7)

Introduction

We report here a novel fluorescent transgenic nude mouse model to visualize angiogenesis of human as well as rodent tumors. We initially reported that nestin, a marker for neural progenitor cells, is also selectively expressed in hair follicle stem cells in nestin-driven green fluorescent protein (ND-GFP) transgenic mouse (1). The ND-GFP hair-follicle stem cells differentiate to form much of the hair follicle each hair growth cycle (1).

We subsequently showed that many of the newly formed blood vessels in the skin of ND-GFP transgenic mice originate from hair follicle cells during the anagen phase (2). The ND-GFP vessels that originate from the hair follicles vascularize the dermis. The

follicular origin of the ND-GFP vessels is most evident when transplanting ND-GFP-labeled follicles to unlabeled nude mice. In the transplanted mice, new fluorescent blood vessels originate only from the labeled follicles. The vessels from the transplanted ND-GFP follicles responded to presumptive angiogenic signals from healing wounds (1).

We recently reported that new blood vessels vascularizing a murine melanoma transplanted to the skin of ND-GFP mice are derived from ND-GFP hair follicles (3).

In the present study, we crossed the ND-GFP-C57/B6 mouse onto the nude background to obtain ND-GFP nude mice. Dual-color fluorescence imaging visualized nascent tumor angiogenesis of various human tumor cell lines expressing red fluorescent protein (RFP) transplanted to the ND-GFP nude mice. We also visualized nascent angiogenesis of an RFP-expressing murine melanoma and breast cancer cell lines transplanted to these mice. The ND-GFP nude mouse is a useful model to visualize tumor angiogenesis and screen for antiangiogenic inhibitors.

Materials and Methods

ND-GFP transgenic nude mice. ND-GFP transgenic C57/B6 mice carry GFP under the control of the nestin second-intron enhancer (1, 2, 4-7). In the present study, the ND-GFP gene was crossed into nude mice on the C57/B6 background to obtain ND-GFP nude mice.

Red fluorescent protein vector production. (8) The *RFP* (DsRed-2) gene (BD Biosciences Clontech, Palo Alto, CA; ref. 9) was inserted in the retroviral-based mammalian expression vector pLNCX (Clontech) to form the pLNCX DsRed-2 vector. Production of retrovirus resulted from transfection of pLNCX DsRed-2 in PT67 packaging cells, which produced retroviral supernatants containing the DsRed-2 gene. Briefly, PT67 cells were grown as monolayers in DMEM supplemented with 10% FCS (Gemini Biological Products, Calabasas, CA). Exponentially growing cells (in 10 cm dishes) were transfected with 10 μ g expression vector using a Lipofectamine Plus (GIBCO-BRL, Grand Island, NY) protocol. Transfected cells were replated 48 hours after transfection and 100 μ g/mL G418 was added 7 hours after transfection. Two days later, the amount of G418 was increased to 200 μ g/mL G418. After 25 days of drug selection, surviving colonies were visualized under fluorescence microscopy and RFP-positive colonies were isolated. Several clones were selected and expanded into cell lines after virus titering on the 3T3 cell line.

RFP gene transduction of tumor cell lines. For *RFP* gene transduction, 20% confluent human and rodent cells were incubated with a 1:1 precipitated mixture of retroviral supernatants of PT67 cells and RPMI 1640 or other culture media (GIBCO) containing 10% fetal bovine serum (Gemini Biological Products) for 72 hours. Fresh medium was replenished at this time. Tumor cells were harvested with trypsin/EDTA and subcultured at a ratio of 1:15 into selective medium, which contained 50 μ g/mL G418. To select brightly fluorescent cells, the level of G418 was increased to 800 μ g/mL in a stepwise manner. Clones expressing RFP were isolated with cloning cylinders (Bel-Art Products) by trypsin/EDTA and were amplified and transferred by conventional culture methods in the absence of selective agent (8).

Requests for reprints: Robert M. Hoffman, AntiCancer Inc., San Diego, CA 92111. Phone: 858-654-2555; Fax: 858-268-4175; E-mail: all@anticancer.com.
©2005 American Association for Cancer Research.

Measurement of length of nestin-positive nascent blood vessels. Angiogenesis was quantified in the tumor tissue by measuring the length of ND-GFP nascent blood vessels in all fields under fluorescence microscopy. All fields at $\times 40$ or $\times 100$ magnification were measured to calculate the total length of ND-GFP-positive nascent blood vessels. The vessel density was calculated by the total length of ND-GFP nascent blood vessels divided by tumor area (3).

Immunohistochemical staining. Colocalization of ND-GFP fluorescence, the endothelial cell marker CD31, and nestin in frozen skin sections of the nestin-GFP transgenic mice was detected with the anti-rat immunoglobulin horseradish peroxidase (HRP) detection kit (BD PharMingen, San Diego, CA; CD31) and the anti-mouse immunoglobulin HRP detection kit (BD PharMingen; nestin) following the instructions of the manufacturer. The primary antibodies used were CD31 monoclonal antibody (mAb; 1:50) and nestin mAb (1:80). Substrate chromogen 3,3'-diaminobenzidine staining was used for antigen staining. Anti-CD31 mAb (CBL1337) was purchased from Chemicon (Temecula, CA). Anti-nestin mAb (rat 40) was purchased from BD PharMingen (2).

Red fluorescent protein or red fluorescent protein-green fluorescent protein human cutaneous fibrosarcoma model. ND-GFP transgenic nude mice, 6 to 8 weeks old, were used. The mice were anesthetized with tribromoethanol. Fifty microliters containing 1×10^6 RFP-expressing or dual-color RFP and GFP-expressing human HT1080 fibrosarcoma cells (8) per mouse were injected in the skin of the ND-GFP mice with a 1 mL 27G1/2 latex-free syringe (Becton Dickinson, Franklin Lakes, NJ). The mice were anesthetized with tribromoethanol, and samples of tumor mass with skin were excised at days 10 and 14 after implantation of tumor cells. The tumor samples with skin were divided into two parts, one for fluorescence microscopy and the other for frozen sections. One tumor sample with skin was observed under fluorescence microscopy. The other tumor sample was embedded in tissue-freezing embedding medium (Triangle Biomedical Sciences, Durham, NC) and frozen at -80°C overnight. Frozen sections of 10 μm thickness were cut with a Leica CM1850 cryostat (Leica, Nussloch, Germany) and were air dried (10).

Red fluorescent protein-expressing murine cutaneous melanoma model. ND-GFP transgenic nude mice, 6 to 8 weeks old, were used. The mice were anesthetized with tribromoethanol (i.p. injection 0.2 mL/10 g body weight of a 1.2% solution). Fifty microliters containing 2×10^6 RFP-expressing B16F10 murine melanoma cells per mouse were injected into the skin of the ND-GFP nude mice with a 1 mL 27G1/2 latex-free syringe (Becton Dickinson). The mice were anesthetized with tribromoethanol. Samples of tumor mass with skin were excised at days 10 and 14 after implantation of tumor cells (11).

Red fluorescent protein-expressing orthotopic murine breast cancer model. ND-GFP transgenic nude mice, 6 to 8 weeks old, were used. The mice were anesthetized with tribromoethanol. Fifty microliters containing 1×10^6 RFP-expressing MMT060562 murine mammary tumor cells per mouse were injected into the mammary fat pad of the ND-GFP mice with a 1 mL 27G1/2 latex-free syringe (Becton Dickinson). On days 10 and 14 after implantation, the mice were anesthetized with tribromoethanol, and tumor samples were excised. The tumor samples were divided into two parts, one for fluorescence microscopy and the other for frozen sections (11).

Red fluorescent protein-expressing orthotopic human brain cancer model. ND-GFP transgenic nude mice, 6 to 8 weeks old, were used as the host for U87-RFP human glioma cell line. Fifty microliters containing 1×10^6 RFP-expressing U87 cells per mouse were injected into the subcutis in 6- to 8-week-old nude mice with a 1 mL 27G1/2 latex-free syringe (Becton Dickinson). Tumor fragments (1 mm³), stably expressing RFP, previously grown s.c. in nude mice, were implanted by surgical orthotopic implantation on the right parietal lobe of the brain in the ND-GFP nude mice. The parietal bone of the skull was exposed following an arc-shaped scalp incision. The tumor pieces were implanted into the right parietal lobe of the brain. The incision in the scalp was closed with a 6-0 surgical suture in one layer. The animals were kept under tribromoethanol anesthesia during surgery. On day 14 after implantation of the tumor, the mice were anesthetized with tribromoethanol. The tumor in the brain was directly observed by

fluorescence microscopy. The tumor mass was then excised. All procedures of the operation described above were done with a $\times 7$ magnification microscope (MZ6, Leica; ref. 12).

Red fluorescent protein-expressing orthotopic human pancreas cancer model. ND-GFP transgenic nude mice, 6 to 8 weeks old, were used as the host for the Bx-PC-3-RFP and MiaPaCa-RFP human pancreas cancer cell lines. Fifty microliters containing 2×10^6 RFP-expressing pancreatic cancer cells per mouse were injected in the subcutis in 6- to 8-week-old nude mice with a 1 mL 27G1/2 latex-free syringe (Becton Dickinson). Tumor fragments (1 mm³), stably expressing RFP, previously grown s.c. in nude mice, were implanted by surgical orthotopic implantation on the pancreas of the ND-GFP nude mice. After proper exposure of the pancreas, 7-0 surgical sutures were used to penetrate the tumor pieces and attach them to the pancreas (13). The incision in the abdominal wall was closed with a 6-0 surgical suture in one layer. The animals were kept under tribromoethanol anesthesia during surgery. On day 14 after implantation of the tumor, the mice were anesthetized with tribromoethanol. The tumor in the pancreas was directly observed by fluorescence microscopy. Tumor samples were excised. All procedures of the operation described above were done with a $\times 7$ magnification microscope (MZ6, Leica). The tumor samples were divided into two parts, one for fluorescence microscopy and the other for frozen sections (13, 14).

Red fluorescent protein-expressing orthotopic human colon cancer model. ND-GFP transgenic nude mice, 6 to 8 weeks old, were used as the host for the HCT-116-RFP human colon cancer cell line. Fifty microliters containing 2×10^6 HCT-116-RFP cells per mouse were injected into the subcutis in 6- to 8-week-old nude mice with a 1 mL 27G1/2 latex-free syringe (Becton Dickinson). Tumor fragments (1 mm³), stably expressing RFP, previously grown s.c. in nude mice, were implanted by surgical orthotopic implantation on the colon of the ND-GFP nude mice. After proper exposure of the colon through a lower-left abdominal incision, 8-0 surgical sutures were used to penetrate the tumor pieces and attach them under the serosa of the ascending colon (15). The incision in the abdominal wall was closed with a 6-0 surgical suture in one layer. The animals were kept under tribromoethanol anesthesia during surgery. On day 14 after implantation of tumor cells, the mice were anesthetized with tribromoethanol. The tumor in the colon was directly observed by fluorescence microscopy, and the samples of the tumor were excised. All procedures of the operation described above were done with a $\times 7$ magnification microscope (MZ6, Leica; refs. 8, 15).

Whole-body imaging. Whole-body imaging was done in a fluorescent light box illuminated by fiber-optic lighting at 470 nm (Lighttools Research, Encinitas, CA). Emitted fluorescence was collected through a long-pass filter GG475 (Chroma Technology, Brattleboro, VT) on a Hamamatsu C5810 three-chip cooled color CCD camera (Hamamatsu Photonics, Bridgewater, NJ). High-resolution images of 1,024/724 pixels were captured directly on an IBM PC. Images were processed for contrast and brightness and analyzed with the use of IMAGE PRO PLUS 3.1 software (Media Cybernetics, Silver Spring, MD; ref. 16).

Fluorescence microscopy. Fluorescence microscopy was carried out using an Olympus IMT-2 inverted microscope equipped with a mercury lamp power supply. The microscope had a GFP filter set (Chroma Technology). Tissue samples were directly observed (17).

Statistical analysis. The experimental data are expressed as the mean \pm SD. Statistical analysis was done using two-tailed Student's *t* test.

Results and Discussion

Characterization of the ND-GFP nude mouse. ND-GFP was expressed in the brain, spinal cord, pancreas, stomach, esophagus, heart, blood vessels of glomeruli, blood vessels of skeletal muscle, testes, hair follicles, and blood vessel network in the skin of the ND-GFP mouse (Fig. 1; Table 1).

Nascent angiogenesis of human fibrosarcoma subcutaneous implanted in the ND-GFP nude mouse. HT1080 human fibrosarcoma cells, expressing histone H2B-GFP in the nucleus and RFP in the cytoplasm (10), were implanted into the subcutis of

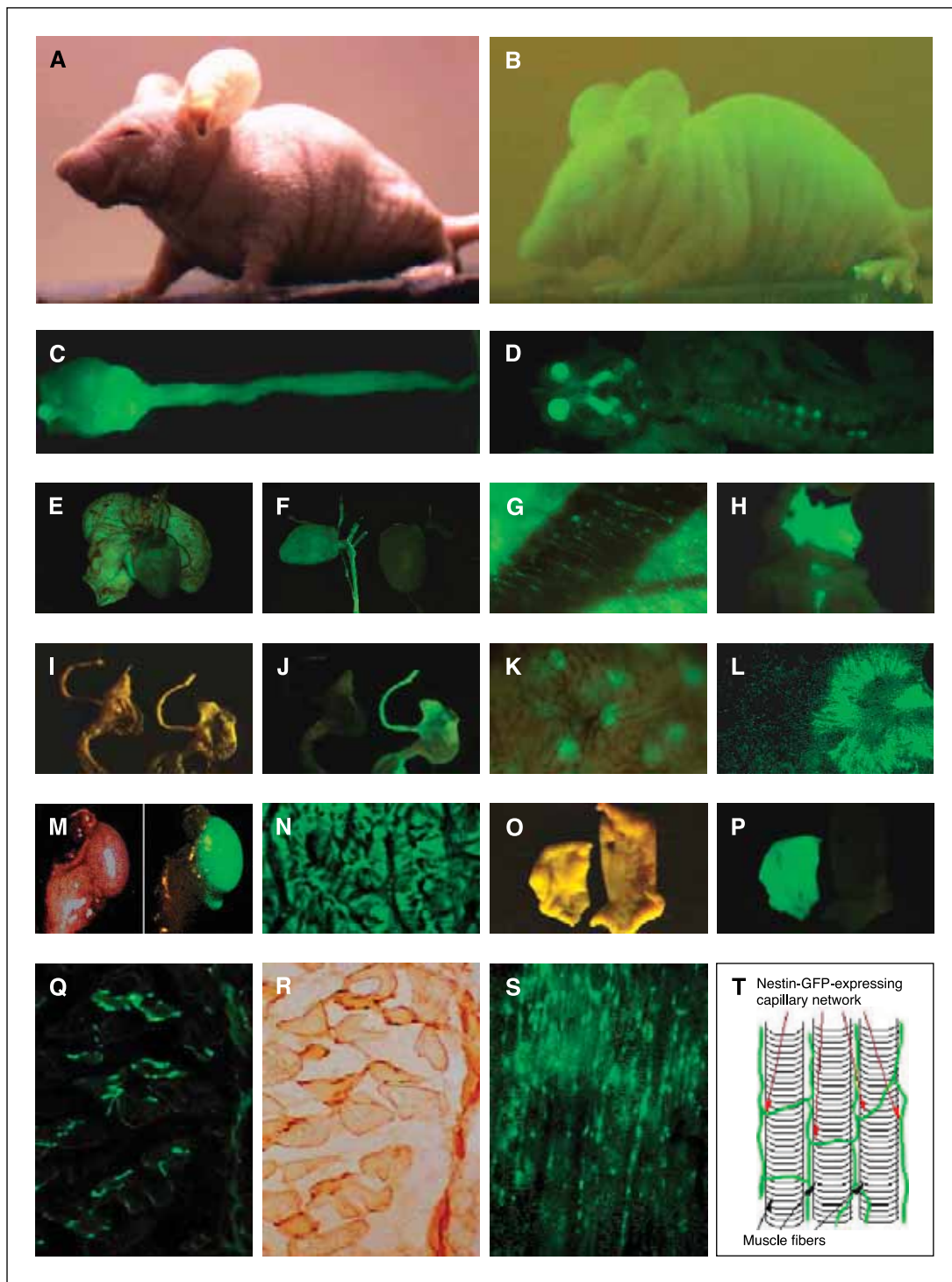


Figure 1. GFP expression in various organs and tissues of transgenic ND-GFP nude mouse. *A*, adult nestin-nude mouse; bright field. *B*, same mouse as in *A*. The mouse is glowing with ND-GFP expression under blue light excitation. *C*, ND-GFP expression in the brain and the spinal cord (dorsal view). *D*, strong ND-GFP expression can be seen in the optic chiasma and the dorsal roots of the spinal cord (dorsal view; the brain and spinal cord were removed). *E*, ND-GFP expression can be detected in the heart and the lungs. *F*, the dissected circulatory system of ND-GFP nude mouse (*left side*), including the heart and major arteries and veins, express ND-GFP. GFP expression could not be detected in the circulatory system of a non-ND-GFP nude mouse (*right side*). *G*, ND-GFP-expressing capillaries in the cardiac vasculature wall. *H*, the pancreas is strikingly glowing with ND-GFP expression. *I*, bright-field image of the esophagus, stomach, and the duodenum of regular nude mouse (*left side*) and that of ND-GFP nude mouse (*right side*). *J*, same as *I*; ND-GFP expression can be visualized in the esophagus, stomach, and the duodenum of the ND-GFP nude mouse (*right*) under blue-light excitation. No GFP fluorescence can be detected in the corresponding organs of the non-ND-GFP nude mouse (*left*). *K*, strong ND-GFP expression can be seen in the glomerulus capillaries of the kidney. *L*, the vasculature of the renal hilum is strikingly glowing with ND-GFP expression. *M*, bright-field (*left side*) and fluorescence-field (*right side*) images of testis and epididymis. The testis is glowing with ND-GFP expression. *N*, ND-GFP-expressing cells around the seminiferous tubules. *O*, bright-field image of the skin of nude non-ND-GFP mouse (*left side*) and that of ND-GFP nude mouse (*right side*). *P*, same as *O*; GFP expression in the skin of ND-GFP nude mouse (*left*) under blue-light excitation. Skin from non-ND-GFP mouse is not fluorescent (*right*). *Q*, frozen section of ND-GFP-expressing blood vessels of the muscle fibers. *R*, same section as *Q*; CD31 is expressed in blood vessels of the muscle fibers. *S*, ND-GFP-expressing blood vessels of the muscle fibers. *T*, cartoon of nestin-GFP-expressing blood vessels of the muscle fibers.

Table 1. ND-GFP–expressing organs and tissues in the ND-GFP nude and ND-GFP C57/B16 mice

Organ	Degree of fluorescence in ND-GFP nude mouse	Comments	Reference
Skin	++++	ND-GFP–expressing hair follicle stem cells are precursors of ND-GFP–expressing hair follicles and network of blood vessels interconnecting the follicles.	Li et al. (1) Amoh et al. (2) Amoh et al. (19) Present work
Brain	+++++	Optic chiasma, neural crest, and neural stem cells were found to express ND-GFP in C57/B6 mice.	Zimmerman et al. (5) Lendahl et al. (4) Lothian and Lendahl (20) Kawaguchi et al. (21) Yamaguchi et al. (22) Yaworsky and Kappen (23) Mignone et al. (7) Present work
Spinal cord	+++		Present work
Pancreas	++++	Islets, ductal epithelia, pericytes, mesenchymal region, vascular endothelial cells, and acinar cells express ND-GFP in C57/B6 mice.	Hunziker and Stein (24) Zulewski et al. (25) Klein et al. (26) Lardon et al. (27) Selander and Edlund (28) Present work
Testis	++++		Frojdman et al. (29) Present work
Skeletal muscle	++	Blood vessels in muscle express ND-GFP.	Sejeren and Lendahl (30) Present work
Kidney	++	Blood vessels in glomerulus express ND-GFP.	Present work
Stomach	++		Present work
Duodenum	+		Present work
Esophagus	+++		Present work
Heart	+		Present work
Lung	++		Present work

the ND-GFP nude mice. On day 14 after implantation of tumor cells, ND-GFP–expressing nascent blood vessels were visualized growing into the dual-color tumor mass. The dual-color tumor cells became polarized toward the ND-GFP–expressing nascent blood vessels (Fig. 2).

Nascent angiogenesis of murine melanoma implanted in the ND-GFP nude mouse. B16F10-RFP growing in the skin had numerous GFP-expressing ND-GFP vessels within the tumor (Fig. 2). The extensive vascularization was striking when only the GFP vessels were visualized (Fig. 2). Doxorubicin (5 $\mu\text{g/g}$ qd \times 3) inhibited the formation of ND-GFP vessels in the B16F10 tumor by \sim 85% (Fig. 2).

Nascent angiogenesis of orthotopically implanted human pancreatic tumor in the ND-GFP nude mouse. ND-GFP–expressing nascent blood vessels vascularized the orthotopically transplanted RFP-expressing Bx-PC-3 and MiaPaCa human pancreatic tumors (Fig. 2). The endothelial cell marker CD31 and ND-GFP fluorescence were both expressed in the newly formed blood vessels growing into the pancreatic tumor.

ND-GFP–expressing nascent blood vessels vascularize orthotopically implanted human RFP colon tumor in the ND-GFP mouse. ND-GFP–expressing nascent blood vessels vascularized

human colon tumor HCT116-RFP (Fig. 2). CD31 and ND-GFP fluorescence were coexpressed in the newly formed ND-GFP–expressing blood vessels in the colon tumor.

ND-GFP–expressing blood vessels vascularize orthotopically implanted murine mammary tumor. ND-GFP expressing blood vessels vascularized an orthotopically implanted murine mammary tumor MMT060562-RFP. The vessels showed extensive tortuosity and heterogeneity (Fig. 2).

ND-GFP–expressing blood vessels vascularize orthotopically implanted human brain tumor. Extensive vascularization by ND-GFP–expressing blood vessels of the orthotopically implanted U87-RFP human glioma was visualized. Many RFP-expressing tumor cells seemed to grow closely associated with the ND-GFP vessels after implantation (Fig. 2).

Brown et al. (18) showed that multiphoton laser scanning microscopy can visualize *VEGF* gene expression linked to GFP in tumors growing in s.c. implanted chambers. In the present study, dual-color fluorescence imaging visualized tumor angiogenesis in ND-GFP transgenic nude mice. Human glioma, pancreatic cancer, colon cancer, and murine mammary melanoma and breast tumors expressing RFP were vascularized by ND-GFP–expressing blood vessels when implanted orthotopically on their respective organs.

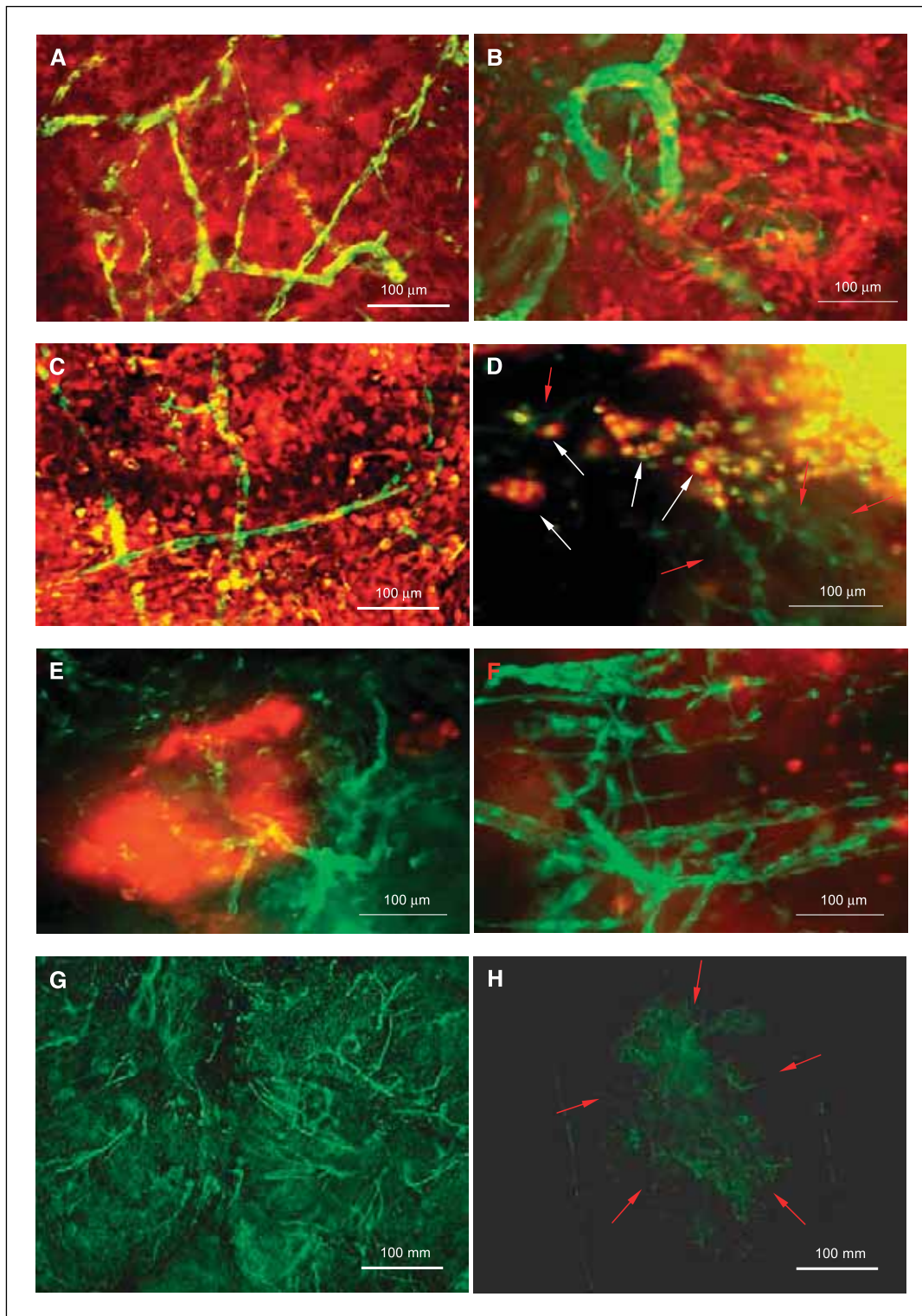


Figure 2. Fluorescence imaging of tumor angiogenesis in transgenic ND-GFP nude mice. *A*, RFP-expressing mouse B16F10 melanoma growing in a nestin-GFP transgenic nude mouse. Host-derived ND-GFP-expressing blood vessels were visualized in the RFP-expressing mouse melanoma on day 10 after s.c. injection of B16F10-RFP cells in the transgenic ND-GFP nude mouse. *Bar*, 100 μ m. *B*, numerous host-derived ND-GFP-expressing blood vessels were visualized in the RFP-expressing mouse mammary tumor on day 14 after orthotopic inoculation of MTT-060562-RFP cells. *Bar*, 100 μ m. *C*, RFP-expressing U87 human glioma growing in the ND-GFP transgenic nude mouse. ND-GFP-expressing blood vessels were visualized in the RFP-expressing human glioma on day 14 after s.c. injection of U87-RFP cells. *Bar*, 100 μ m. *D*, human HT1080 fibrosarcoma on day 14 after injection. Dual-color tumor cells expressing GFP in the nucleus and RFP in the cytoplasm are polarized towards ND-GFP-expressing blood vessels (*white arrows*). *Bar*, 100 μ m. *E*, RFP-expressing Bx-PC-3 human pancreatic tumor vascularized with ND-GFP vessels on day 14 after orthotopic implantation. *Bar*, 100 μ m. *F*, RFP-expressing human HCT-116 colon tumor vascularized with ND-GFP vessels on day 14 after orthotopic implantation. *Bar*, 100 μ m. *G*, extensive ND-GFP-expressing blood vessels were visualized in the RFP-expressing human fibrosarcoma 8 days after injection of HT1080 cells. Only ND-GFP vessels are visualized. *Bar*, 100 mm. *H*, extensive inhibition of ND-GFP-expressing blood vessel formation in the RFP-expressing HT-1080 human fibrosarcoma by 5 μ g/g doxorubicin (i.p.) on days 0, 1, and 2. *Bar*, 100 mm.

Human fibrosarcoma was vascularized by ND-GFP vessels in the skin. Doxorubicin had a strong inhibitory effect on ND-GFP tumor angiogenesis.

The ND-GFP nude mouse model should be useful for the visualization of tumor angiogenesis and evaluation of angiogenetic inhibitors especially in the most important early stages of tumor growth and metastasis.

Acknowledgments

Received 3/10/2005; accepted 4/7/2005.

Grant support: National Cancer Institute grants CA099258, CA103563, and CA101600 to AntiCancer, Inc. NIH grant R21 CA109949-01 and American Cancer Society grant RSG-05-037-01-CCE to M. Bouvet.

The costs of publication of this article were defrayed in part by the payment of page charges. This article must therefore be hereby marked *advertisement* in accordance with 18 U.S.C. Section 1734 solely to indicate this fact.

References

- Li L, Mignone J, Yang M, et al. Nestin expression in hair follicle sheath progenitor cells, *Proc Natl Acad Sci U S A* 2003;100:9958–61.
- Amoh Y, Li L, Yang M, et al. Nascent blood vessels in the skin arise from nestin-expressing hair-follicle cells. *Proc Natl Acad Sci U S A* 2004;101:13291–5.
- Amoh Y, Li L, Yang M, et al. Hair-follicle-derived blood vessels vascularize tumors in skin and are inhibited by doxorubicin. *Cancer Res* 2005;65:2337–43.
- Lendahl U, Zimmerman LB, McKay RD. CNS stem cells express a new class of intermediate filament protein. *Cell* 1990;60:585–95.
- Zimmerman L, Parr B, Lendahl U, et al. Independent regulatory elements in the nestin gene direct transgene expression to neural stem cells or muscle precursors. *Neuron* 1994;12:11–24.
- Yaworsky PJ, Kappen C. Heterogeneity of neural progenitor cells revealed by enhancers in the nestin gene. *Dev Biol* 1999;205:309–21.
- Mignone JL, Kukekov V, Chiang AS, Steindler D, Enikolopov G. Neural stem and progenitor cells in nestin-GFP transgenic mice. *J Comp Neurol* 2004;469:311–24.
- Yang M, Reynoso J, Jiang P, et al. Transgenic nude mouse with ubiquitous green fluorescent protein expression as a host for human tumors. *Cancer Res* 2004;64:8651–6.
- Matz MV, Fradkov AF, Labas YA, et al. Fluorescent proteins from nonbioluminescent Anthozoa species. *Nat Biotechnol* 1999;17:969–73.
- Yamamoto N, Jiang P, Yang M, et al. Cellular dynamics visualized in live cells *in vitro* and *in vivo* by differential dual-color nuclear-cytoplasmic fluorescent-protein expression. *Cancer Res* 2004;64:4251–6.
- Yang M, Li L, Jiang P, et al. Dual-color fluorescence imaging distinguishes tumor cells from induced host angiogenic vessels and stromal cells. *Proc Natl Acad Sci U S A* 2003;100:14259–62.
- Yang M, Baranov E, Wang J-W, et al. Direct external imaging of nascent cancer, tumor progression, angiogenesis, and metastasis on internal organs in the fluorescent orthotopic model. *Proc Natl Acad Sci U S A* 2002;99:3824–9.
- Fu X, Guadagni F, Hoffman RM. A metastatic nude-mouse model of human pancreatic cancer constructed orthotopically with histologically intact patient specimens. *Proc Natl Acad Sci U S A* 1992;89:5645–9.
- Katz MH, Takimoto S, Spivack D, et al. A novel red fluorescent protein orthotopic pancreatic cancer model for the preclinical evaluation of chemotherapeutics. *J Surg Res* 2003;113:151–60.
- Fu X, Besterman JM, Monosov A, Hoffman RM. Models of human metastatic colon cancer in nude mice orthotopically constructed by using histologically intact patient specimens. *Proc Natl Acad Sci U S A* 1991;88:9345–9.
- Yang M, Baranov E, Jiang P, et al. Whole-body optical imaging of green fluorescent protein-expressing tumors and metastases. *Proc Natl Acad Sci U S A* 2000;97:1206–11.
- Chishima T, Miyagi Y, Wang X, et al. Cancer invasion and micrometastasis visualized in live tissue by green fluorescent protein expression. *Cancer Res* 1997;57:2042–7.
- Brown EB, Campbell RB, Tszuki Y, et al. *In vivo* measurement of gene expression, angiogenesis and physiological function in tumors using multiphoton laser scanning microscopy. *Nat Med* 2001;7:864–8.
- Amoh Y, Li L, Katsuoka K, Penman S, Hoffman RM. Multipotent nestin-positive, keratin-negative hair-follicle bulge stem cells can form neurons. *Proc Natl Acad Sci U S A* 2005;102:5530–4.
- Lothian C, Lendahl U. An evolutionarily conserved region in the second intron of the human nestin gene directs gene expression to CNS progenitor cells and to early neural crest cells. *Eur J Neurosci* 1997;9:452–62.
- Kawaguchi A, Miyata T, Sawamoto K, et al. Nestin-EGFP transgenic mice: visualization of the self-renewal and multipotency of CNS stem cells. *Mol Cell Neurosci* 2001;17:259–73.
- Yamaguchi M, Saito H, Suzuki M, Mori K. Visualization of neurogenesis in the central nervous system using nestin promoter-GFP transgenic mice. *Neuroreport* 2000;11:1991–6.
- Yaworsky PJ, Kappen C. Heterogeneity of neural progenitor cells revealed by enhancers in the nestin gene. *Dev Biol* 1999;205:309–21.
- Hunziker E, Stein M. Nestin-expressing cells in the pancreatic islets of Langerhans. *Biochem Biophys Res Commun* 2000;271:116–9.
- Zulewski H, Abraham EJ, Gerlach MJ, et al. Multipotential nestin-positive stem cells isolated from adult pancreatic islets differentiate *ex vivo* into pancreatic endocrine, exocrine, and hepatic phenotypes. *Diabetes* 2001;50:521–33.
- Klein T, Ling Z, Heimberg H, Madsen OD, Heller RS, Serup P. Nestin is expressed in vascular endothelial cells in the adult human pancreas. *J Histochem Cytochem* 2003 Jun;51:697–706.
- Lardon J, Rooman I, Bouwens L. Nestin expression in pancreatic stellate cells and angiogenic endothelial cells. *Histochem Cell Biol* 2002;117:535–40.
- Selander L, Edlund H. Nestin is expressed in mesenchymal and not epithelial cells of the developing mouse pancreas. *Mech Dev* 2002;113:189–92.
- Frojdman K, Pelliniemi LJ, Lendahl U, Virtanen I, Eriksson JE. The intermediate filament protein nestin occurs transiently in differentiating testis of rat and mouse. *Differentiation* 1997;61:243–9.
- Sejersens T, Lendahl U. Transient expression of the intermediate filament nestin during skeletal muscle development. *J Cell Sci* 1993;106:1291–300.